

2009-01-01

## Integration of Microstrip Patch Antennas with Polycrystalline Silicon Solar Cells

S. Shynu

*Technological University Dublin*

Maria Roo Ons

*Technological University Dublin*

Max Ammann

*Technological University Dublin, max.ammann@tudublin.ie*

Sarah McCormack

*Technological University Dublin*

Brian Norton

*Technological University Dublin, brian.norton@tudublin.ie*

Follow this and additional works at: <https://arrow.tudublin.ie/dubenart>



Part of the [Engineering Commons](#)

### Recommended Citation

Shynu, S. et al (2006) Integration of Microstrip Patch Antennas with Polycrystalline Silicon Solar Cells. *IEEE Transactions on Antennas and Propagation*, vol. 37, no. 12, pp. 3969-3922. doi:10.1109/TAP.2009.2026438.

This Article is brought to you for free and open access by the Dublin Energy Lab at ARROW@TU Dublin. It has been accepted for inclusion in Articles by an authorized administrator of ARROW@TU Dublin. For more information, please contact [yvonne.desmond@tudublin.ie](mailto:yvonne.desmond@tudublin.ie), [arrow.admin@tudublin.ie](mailto:arrow.admin@tudublin.ie), [brian.widdis@tudublin.ie](mailto:brian.widdis@tudublin.ie).



This work is licensed under a [Creative Commons Attribution-NonCommercial-Share Alike 3.0 License](#)

# Communications

## Integration of Microstrip Patch Antenna With Polycrystalline Silicon Solar Cell

S. V. Shynu, Maria Jose Roo Ons, Patrick McEvoy, Max J. Ammann, Sarah J. McCormack, and Brian Norton

**Abstract**—The implementation of a polycrystalline silicon solar cell as a microwave groundplane in a low-profile, reduced-footprint microstrip patch antenna design for autonomous communication applications is reported. The effects on the antenna/solar performances due to the integration, different electrical conductivities in the silicon layer and variation in incident light intensity are investigated. The antenna sensitivity to the orientation of the anisotropic solar cell geometry is discussed.

**Index Terms**—Integration, microstrip antenna, solar antenna, solar cells.

### I. INTRODUCTION

Remote terrestrial systems that communicate tracking, telemetry or control information via a wireless microwave link can be sustained autonomously with solar energy. In these designs, the communications antenna is typically displaced from the panels of photovoltaic cells [1] to minimize inefficiency due to structural shadows. However, the integration of the solar cell and the antenna into a single device can provide a more compact surface area for smaller systems. Accordingly, various configurations have been suggested to minimize degradation in both the solar and the microwave performances [2]–[6]. The first reported integration superimposed solar cells of an unspecified silicon (Si) type onto a 2.225 GHz microstrip patch [2]. A separation distance of 5.5 mm was maintained from the perimeter of the solar cells to the radiating patch edges in order to minimize suppression of the electric fields. An increased measure of integration and an enhanced solar cell overlay was achieved with amorphous-Si (a-Si) grown directly on the groundplane of a 4.1 GHz stainless steel slot antenna [3]. Subsequent development of an a-Si cell on a flexible thin film polymer substrate yielded an improved photovoltaic performance at lower cost.

The concept of stimulating radiation directly from a GaAs solar cell at 2.75 GHz is reported in [4] and the application performance of a monocrystalline Si (mono-Si) solar cell as a 1.575 GHz GPS antenna is detailed in [5]. The microwave energy was aperture coupled into the solar cell for radiation for each design. In a third innovative approach, the microstrip groundplane was substituted by a standard Si solar cell underneath a metallodielectric reflect-array of crossed-dipoles for an 8.5 GHz horn-reflector antenna [6]. The impaired RF efficiency was attributed to difficulties in characterizing the electrical properties of

Manuscript received October 06, 2008; revised May 11, 2009. First published June 30, 2009; current version published December 01, 2009. This work was supported by Science Foundation Ireland under Grant 05/RF/ENE025.

S. V. Shynu, M. J. Roo Ons, P. McEvoy, and M. J. Ammann are with Antenna and High Frequency Research Centre, School of Electronic and Communications Engineering, Dublin Institute of Technology, Dublin, Ireland (e-mail: shynunair@gmail.com; mariajose.roons@student.dit.ie; Patrick.McEvoy@dit.ie; ammann@ieee.org).

S. McCormack and B. Norton are with Dublin Energy Lab, Focas Institute, Dublin Institute of Technology, Dublin, Ireland (e-mail: sarah.mccormack@dit.ie; brian.norton@dit.ie).

Digital Object Identifier 10.1109/TAP.2009.2026438

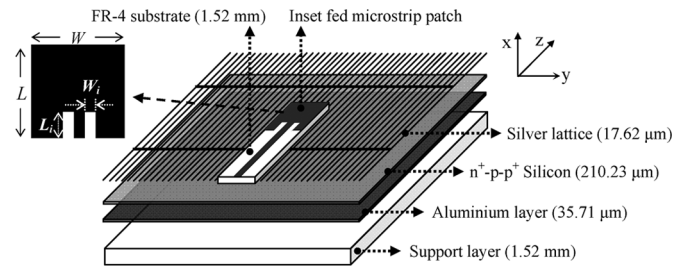


Fig. 1. Exploded layout of the solar antenna geometry and co-ordinate system.

the micron-scale features of the solar cell and the consequent impediments to the antenna optimization. More recently, a polycrystalline-Si (poly-Si) solar cell groundplane below a 2 GHz quarter-wave shorted metal plate antenna maintained 96.54% of its photovoltaic output despite the shadow-casting of the 10 mm profile [7]. The performance of printed antennas over solar cell groundplanes will largely depend on disruption of the microwave surface-currents by the photovoltaic component.

Standard poly-Si solar cells are available with solar energy efficiencies (> 15%) that approach those of mono-Si (> 18%) but with a significant lower cost [8]. The photosensitive poly-Si layer is partially masked by a cathode lattice of silver (Ag) electrodes with orthogonal bus bars on the front side and it interfaces with a homogeneous aluminum (Al) anode layer on the rear side. The anisotropic structure of the Ag-lattice corresponds with increased conductivity in the  $n^+$  semiconductor regions in the extrinsic poly-Si. The differing conductivities and the higher permittivity Si create an inhomogeneous medium between the antenna substrate and the homogenous Al contact layer.

This communication reports simulation and measurement results that characterize the inhomogeneous influences of a poly-Si solar cell groundplane for a printed microwave microstrip antenna. Applications that use of this type of integrated device would require stable antenna radiation characteristics during varying lighting conditions for the solar cell.

### II. MICROSTRIP PATCH SOLAR ANTENNA

Simulations with CST's Microwave Studio were initially used to analyze and optimize the antenna performance above the solar cell groundplane. The structure, shown in Fig. 1, comprises a printed microstrip patch antenna on single-sided FR-4 substrate, of height = 1.52 mm and  $\epsilon_r = 4.2$ , with a  $50 \Omega$  inset feed line in order to avoid piercing the brittle solar cell. The SMA port is grounded to the Al layer of the solar cell. In order to minimize light shadow on the solar cell, the FR-4 substrate is truncated at the edges of the antenna features. The square patch dimensions are  $L = W = 33.62$  mm and the feed-inset parameters of  $L_i = 9$  mm and  $W_i = 3$  mm. The 3 mm wide feedline has a 61.62 mm length in order to place the patch over the center of the poly-Si cell.

A poly-Si solar cell from *Solland*, with dimensions  $156 \times 156 \times 0.26$  mm was selected and measurements were carried out with a Reichert-Jung MeF3 metallurgical microscope to establish the layer dimensions. On the upper surface, the Ag-lattice layer is  $17.62 \mu\text{m}$  thick. It comprises 57 electrodes with a line width and separation of 0.1 mm and 2.64 mm respectively, and 2 orthogonally oriented bus bars that are

TABLE I  
SUMMARY OF SIMULATED AND MEASURED SOLAR ANTENNA PARAMETERS FOR VARIOUS GROUNDPLANE CONFIGURATIONS

Integrated Configuration	Minimum $S_{11}$ Frequency (GHz)		-10 dB Bandwidth (%)		Peak Gain $\{\theta = 90^\circ\}$ (dBi)	
	Simulated	Measured	Simulated	Measured	Simulated	Measured
Homogenous Cu Layer	2.274	2.276	2.43	2.42	3.04	2.60
Si / Parallel Ag-Lattice	2.190	2.190	3.13	3.11	1.86	1.23
Si / Perpendicular Ag-Lattice	2.169	2.168	3.30	3.13	1.55	1.05
Si without Ag-Lattice	2.160	n/a	3.40	n/a	1.24	n/a

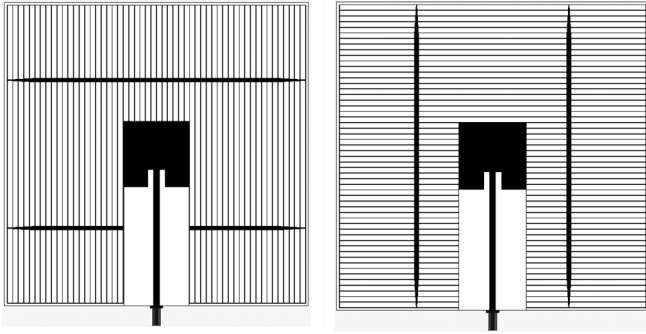


Fig. 2. Electrode lines alignment with the microstrip feed line: parallel (left) and perpendicular (right).

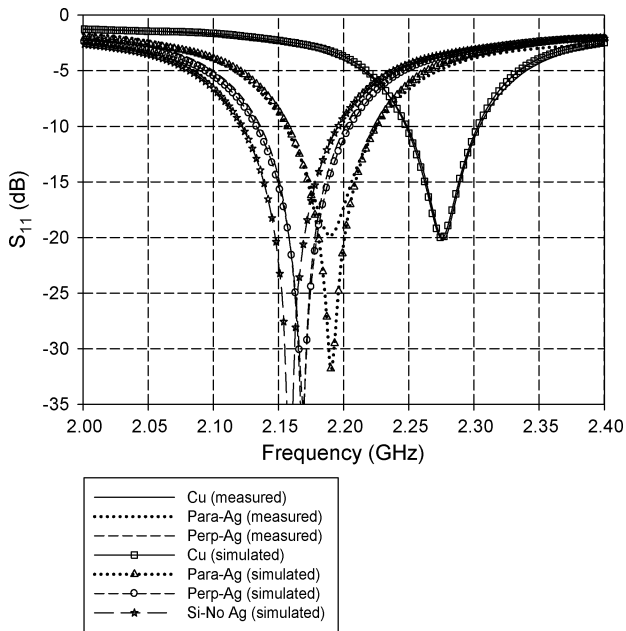


Fig. 3. Simulated and measured  $S_{11}$  for the solar antenna configurations.

2 mm wide and separated by 74.18 mm. The  $n^+ - p - p^+$  doped poly-Si layer thickness is 210.23  $\mu\text{m}$  and the lower Al contact layer thickness is 35.71  $\mu\text{m}$ . Fracturing the brittle poly-Si solar cell was prevented by supporting the integrated structure on a thin dielectric layer.

The  $n^+ - p - p^+$  doped regions of the poly-Si substrate were modeled with a bulk permittivity  $\epsilon_r = 15.3$  and conductivities were set in proportion to the ambient light intensity and temperature of the laboratory, 1.4  $\text{W m}^{-2}$  and 293 K respectively. The conductivity values are

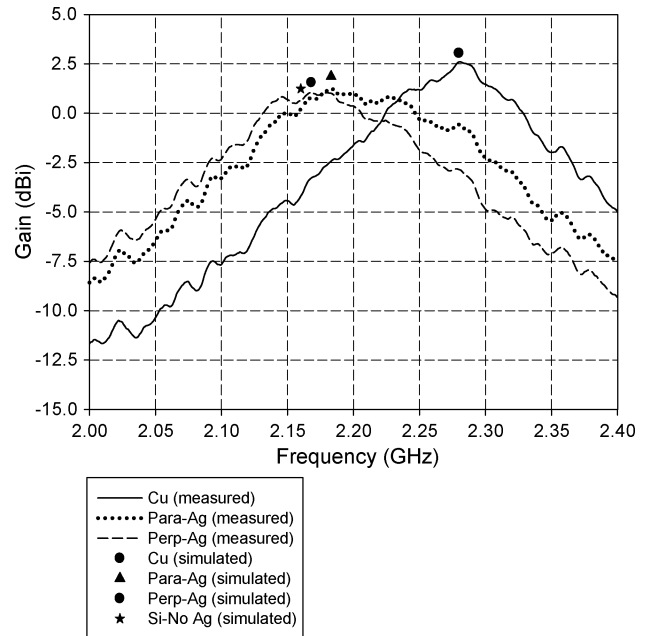


Fig. 4. Simulated and measured gain for the solar antenna configurations.

$\sigma = 254,383 \text{ S m}^{-1}$  for the light exposed area and  $\sigma = 310 \text{ S m}^{-1}$  for the FR-4 shaded area [9].

### III. INHOMOGENEOUS GROUNDPLANE INVESTIGATION

For a conventional half-wave microstrip patch design, the resonant electric near-fields radiate from the antenna feed edge, and opposite edge, to the groundplane through the substrate. The orientation of the anisotropic Ag-lattice (shown in Fig. 2) with respect to the electric near-fields, was anticipated to be significant to the integrated radiating performance. The field flux lines from radiating edges of the truncated substrate patch are typically parallel with the microstrip feed which is used as an orientation reference. To interpret the impact of the inhomogeneous conducting groundplane below the truncated FR-4 substrate; the antenna feed line was aligned: (1) parallel with the Ag electrode lines; (2) perpendicular with the Ag electrode lines; (3) simulated over Si without the Ag-lattice; and (4) contrasted with a homogenous copper (Cu) groundplane.

### IV. RESULTS AND DISCUSSION

Figs. 3, 4 illustrate the  $S_{11}$  and gain results for the four configurations. The homogeneous groundplane reference is resonant at 2.276 GHz with the highest gain of 2.60 dBi. The -10 dB matched bandwidth is 2.42%. In contrast, a Si groundplane with parallel Ag electrode lines tunes lower to 2.190 GHz and has a gain of 1.23 dBi.

TABLE II  
SUMMARY OF SIMULATED GAINS FOR VARIOUS GROUNDPLANE CONFIGURATIONS

Integrated Configuration	Antenna Gain { $\theta = 90^\circ$ } (dBi)	Transmission Line Losses (dB)	Radiated Gain { $\theta = 90^\circ$ } (dBi)	Gain Difference to Homogenous Cu Layer (dB)
Homogenous Cu Layer	3.04	0.47	2.57	0
Si / Parallel Ag-Lattice	1.86	0.62	1.24	-1.33
Si / Perpendicular Ag-Lattice	1.55	0.65	0.90	-1.67
Si without Ag-Lattice	1.24	0.70	0.54	-2.03

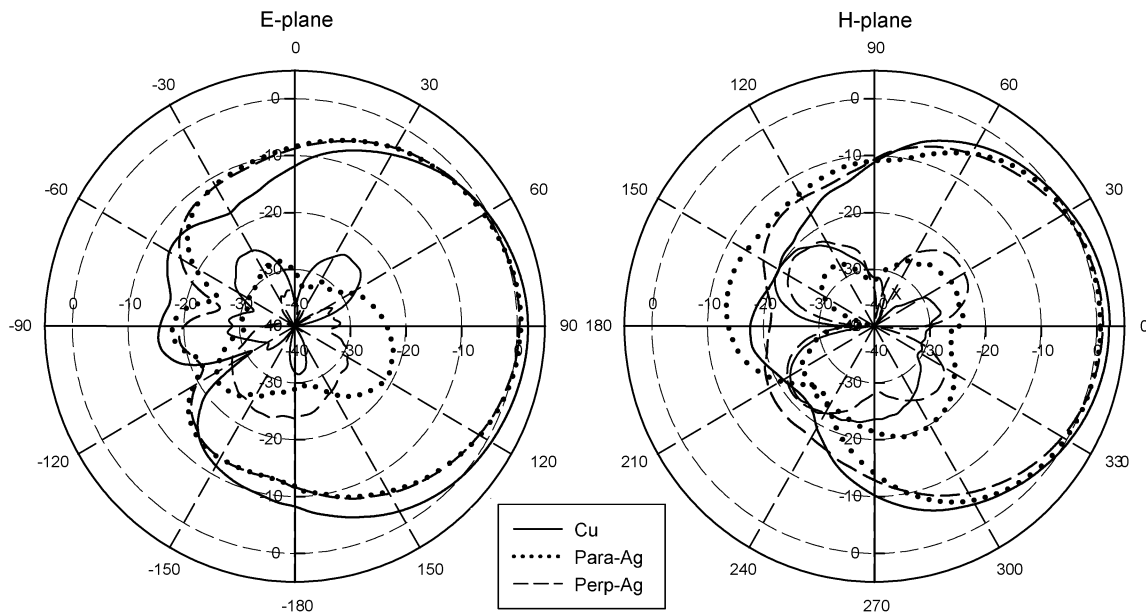


Fig. 5. Measured radiation patterns for the two Ag-bus bar orientations and PEC antenna.

The corresponding bandwidth is 3.11%. Similarly, the perpendicular Ag electrode lines produce an even lower resonance at 2.168 GHz with a reduction in gain to 1.05 dBi and an increase in bandwidth to 3.13%. Table I is a summary comparison of the simulated and measured antenna parameters.

The reductions in gain and the increases in matched bandwidth are evidence for increased losses due to the Si properties. While both Ag-lattice orientations mitigate energy lost in the Si, the perpendicular orientation provides the least isolation. In this case, simulations show that more energy appears at the boundary of the Si and the Al sub-layer. Similarly, the Si permittivity increases the effective dielectric loading for the patch and the resultant downward shift in resonant frequency is more notable for the perpendicular Ag-lattice case. Although measurements were not possible, the simulated removal of the Ag-lattice from a solar cell groundplane indicates that additional energy would be lost in the Si layer. In order to separate the effects of the various groundplane configurations on the feedline, Table II illustrates the simulated antenna gain changes. The changes in gain due to the Si groundplanes are predominantly due to the antenna element interaction with the inhomogeneous substrates.

The parallel Ag electrode lines are in line with the current flow. Although the perpendicular lines are normal to the current flow, the modes are supported because the periodicity of the lines,  $d = 2.64$  mm, is much less than the antenna wavelength,  $\lambda_a = 138$  mm.

The E- and H-plane radiation gain patterns for each of the Ag-lattice orientations are shown in Fig. 5. While the parallel and perpendicular

orientated Si groundplanes lose small amounts in peak gain values, the radiation patterns are similar to the homogeneous Cu case. Cross-polarization isolation values exceeding 20 dB on boresight are observed for both orientations of the Ag-lattice. The similar gain patterns for each of the measured planes and provisional modeling indicates that circularly polarized antennas would perform well provided the periodicity of the Ag-lattice layer is much smaller than the antenna wavelength.

The electrical conductivity in the Si layer of a solar cell increases with more light intensity. Fig. 6 shows the measured  $S_{11}$  and gain for the parallel Ag electrode line configuration with different intensities from a 1 kW solar light simulator in an anechoic chamber. The conductivity of the shaded area under the FR-4 remains stable for the antenna performance. The power produced by the solar cell is proportional to the incident light intensity and is independent of DC loading. Solar cell DC loads ranging from 0–220  $\Omega$  were found to have no effect on the antenna performance. From the photovoltaic point of view, the shaded area due to the microstrip substrate reduces the solar cell efficiency. However, the 13.3 cm<sup>2</sup> FR-4 substrate is only 5.5% of the solar cell area and the measured solar cell efficiency was found to be 12.3%.

## V. CONCLUSION

The implementation of a polycrystalline silicon solar cell as a microwave groundplane for a 2.19 GHz microstrip patch antenna design with a low-profile and reduced-footprint is reported. Measurements and simulations show that the integration provides acceptable antenna/solar

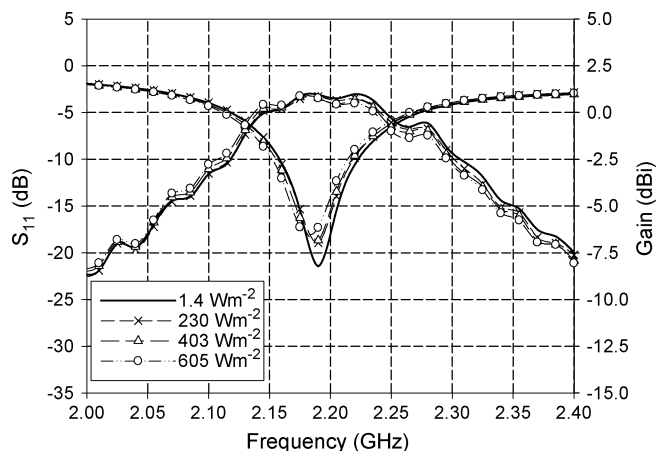


Fig. 6. Variations of parallel solar antenna  $S_{11}$  and Gain with different light intensity values.

cell performance. The reduction in gain is attributed to increased conductivity losses due to the semiconductor properties of the silicon. An anisotropic electrode lattice of silver mitigates some of the losses when the antenna polarization is suitable aligned. The antenna stability is insensitive to light intensity variations typical of countries at northern latitudes.

## REFERENCES

- [1] X. Jiang, J. Polastre, and D. Culler, "Perpetual environmentally powered sensor networks," in *Proc. 4th Int. Symp. Inf. Processing in Sensor Networks*, Los Angeles, CA, Apr. 15, 2005, pp. 463–468.
- [2] M. Tanaka, Y. Suzuki, K. Araki, and R. Susuki, "Microstrip antennas with solar cells for microsattellites," *Electron. Lett.*, vol. 31, no. 1, pp. 5–6, 1995.
- [3] S. Vaccaro, P. Torres, J. R. Mosig, A. Shah, J.-F. Zürcher, A. K. Skrivervik, P. de Maagt, and L. Gerlach, "Stainless steel slot antenna with integrated solar cells," *Electron. Lett.*, vol. 36, no. 25, pp. 2059–2060, 2000.
- [4] S. Vaccaro, J. R. Mosig, and P. de Maagt, "Making planar antennas out of solar cells," *Electron. Lett.*, vol. 38, no. 17, pp. 945–947, 2002.
- [5] N. Henze, A. Giere, H. Fruchting, and P. Hofmann, "GPS patch antenna with photovoltaic solar cells for vehicular applications," in *Proc. IEEE Veh. Technol. Conf. VTC 2003*, Orlando, FL, Oct. 2003, vol. 1, pp. 50–54.
- [6] M. Zawadzki and J. Huang, "Integrated RF antenna and solar array for spacecraft application," in *Proc. IEEE Phased Array Systems and Technol. Conf.*, Dana Point, CA, May 2000, pp. 239–242.
- [7] S. V. Shynu., M. J. Ammann, and B. Norton, "A quarterwave metal plate solar antenna," *IET Electron. Lett.*, vol. 44, no. 9, pp. 570–571, 2008.
- [8] L. L. Kazmerski, "Photovoltaics R&D in the United States: Positioning for our future," in *Proc. 29th IEEE Photovoltaic Specialists Conf.*, New Orleans, LA, May 2002, pp. 21–27.
- [9] U. A. Elani, M. S. Al-Salhi, S. A. Kamh, and J. M. Al-Otaibi, "The conductivity modulation of silicon samples under dark and gamma irradiation conditions," *Solar Energy*, vol. 78, pp. 23–29, 2005.

## Analytical Calculation of Impedance Matching for Probe-Fed Microstrip Patch Antennas

Majid Manteghi

**Abstract**—The goal of this article is to present an analytical solution to the feeding mechanism for a microstrip patch antenna fed by a vertical probe. The feeding mechanism employs a circular capacitive structure to improve the impedance matching, specifically for microstrip patch antennas on thick dielectrics. A circuit model is introduced to find the design parameters. The circuit model includes a series inductor associated with the feeding probe, a parallel plate radial microstrip line, a series radial gap capacitor and an RLC resonator as the patch antenna. A closed form impedance transformation is generated for the parallel plate radial microstrip line. The result of a Schwarz-Christoffel mapping is used to find the radial gap capacitor. The full-wave simulation and measured results are compared with the model and display good agreement.

**Index Terms**—Antenna feeds, broadband antennas, microstrip antennas.

## I. INTRODUCTION

Microstrip patch antennas are known to have a narrow impedance bandwidth. Several techniques have been introduced to improve the bandwidth of microstrip patch antennas [1]–[3]. Most of these attempts to increase bandwidth also increase the cross polarization. However, a pure linear polarization is imperative in many applications, especially those seeking circular polarizations. There is interest in two-port circularly polarized microstrip patch antennas for circular polarizations. There have been many efforts to reduce the cross polarization and achieve wideband performance [4]–[6]. One of the most common approaches to increase the bandwidth of a microstrip patch antenna and avoid cross polarization is to increase the substrate thickness. It has been shown that the bandwidth of a microstrip patch antenna is a linear function of its dielectric thickness [7].

Increasing the bandwidth of the patch antenna with a thicker dielectric substrate also increases the series inductance. Consider the circuit model the input impedance of a probe fed microstrip patch antenna [8] shown in Fig. 1. The input impedance of a patch antenna is modeled as an RLC resonator near its resonant frequency. The series inductor represents the feeding probe, and is proportional to the thickness of the dielectric. One way to reduce the series inductance for a thick substrate is to use a thick feeding probe [9]. Unfortunately, this technique usually has practical problems. Specifically, using a thick probe in the structure of a patch antenna, on a ceramic substrate, imposes mechanical challenges to the design. Adding a thick probe increases the price of the antenna as well. Avoiding the need for a thick probe has advantages. This communication presents a feeding structure which allows the use of a thicker substrate and thus increased bandwidth without added cross polarization, and does not use a thick probe.

The novel feeding mechanism, introduced in [10], is used in this communication. A thin, 1 mm diameter, via is used as the feeding probe of a patch on a 12 mm thick dielectric. The inductance produced by the thin probe is compensated by using a parallel plate radial microstrip line and a series radial gap capacitor. The proposed antenna is illustrated in

Manuscript received May 13, 2008; revised February 20, 2009. First published October 02, 2009; current version published December 01, 2009.

The author is with the Bradley Department of Electrical and Computer Engineering, Virginia Institute of Technology, Blacksburg, VA 24060 USA (e-mail: manteghi@vt.edu).

Color versions of one or more of the figures in this communication are available online at <http://ieeexplore.ieee.org>.

Digital Object Identifier 10.1109/TAP.2009.2033481